Available online at www.sciencedirect.com

jmr&t Journal of Materials Research and Technology

www.jmrt.com.br

Review Article

Ablation behavior and mechanism analysis of C/SiC composites

Yang Wang[a,b], Zhaofeng Chen[a,*], ShengJie Yu[a]

[a] International Laboratory for Insulation and Energy Efficiency Materials, College of Materials Science and Technology, Nanjing University of Aeronautics and Astronautics, Nanjing, China

[b] Suzhou Superlong Aviation Heat Resistance Material Technology Co., Ltd., Suzhou, China

ARTICLE INFO

Article history:
Received 3 June 2015
Accepted 26 October 2015
Available online 26 January 2016

Keywords:
C/SiC composites
Ablation behavior
Ablation mechanism

ABSTRACT

Ablation is an erosive phenomenon with removal of material by a combination of thermo-mechanical, thermo-chemical, and thermo-physical factors with high temperature, pressure, and velocity of combustion flame. Materials with outstanding thermo-mechanical and thermo-chemical properties are required for future high-temperature components. C/SiC is a kind of great potential high-temperature structural material in aeronautics and astronautics with low specific weight, high specific strength, good thermal stability, oxidation resistance and excellent resistance to ablation. In this paper, the ablation phenomenon and mechanisms were summarized adequately. The ablated surface of C/SiC composites could be divided into three regions from center to external. In general, the higher the density, the lower the ablation rate; the lower the ablation temperature and less time, the lower the ablation rate, and the preparation methods also had a great influence on the ablation property. Thermo-physical and thermo-mechanical attacks were the main ablation behavior in the center region; oxidation was the main ablation behavior in the transition region and the border oxidation region.

Yang Wang is Chinese, was born in 1989. He has a bachelor degree in Materials Science and Engineering College of Materials Science and Technology, Nanchang Hangkong University, Nanchang, China in 2012 and Master degree in College of Materials Science and Technology, Nanjing University of Aeronautics and Astronautics, Nanjing, China, obtained in 2014. He is a doctorate student of Nanjing University of Aeronautics and Astronautics now. His main work is in the preparation of high temperature thermal insulation ceramic matrix composite materials including C/C, C_f/SiC, SiC_f/SiC.

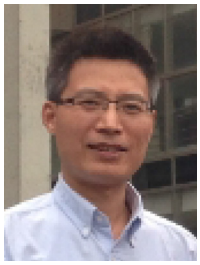

Zhaofeng Chen is Chinese and has a bachelor degree in welding process (1992) and a Master and Doctor degree (2002) in ceramic matrix composite material, from Northwestern Polytechnical University. He acted as professor in College of Materials Science and Technology, Nanjing University of Aeronautics and Astronautics (2008). Zhaofeng Chen is mainly engaged on research of C/C, C/Si_3N_4, C/SiC

* *Corresponding author.*
E-mail: zhaofeng_chen@163.com (Z. Chen).

http://dx.doi.org/10.1016/j.jmrt.2015.10.004

composites and thermal insulation materials for 16years with four scientific research fund project. He has published 38 academic papers (SCI) and has obtained 15 patents.

Shengjie Yu is Chinese, was born in 1990. He has a bachelor's and Master's degree in College of Materials Science and Technology, Nanjing University of Aeronautics and Astronautics, Nanjing, China, obtained in 2013 and 2015, respectively. Actually, he is a doctorate student of Nanjing University of Aeronautics and Astronautics now. His main work is preparation and analysis of ceramic coating and fiber reinforced ceramic matrix composites (FRCMCs), including C/C, C_f/SiC, SiC_f/SiC.

1. Introduction

Materials are the base for technology and advanced technology also requires advanced materials. Ablation is an erosive phenomenon with the removal of material by a combination of thermo-mechanical, thermo-chemical, and thermo-physical factors with high temperature, pressure, and velocity of combustion flame. The effect of fire on organic matrix composites has been widely discussed [1–10]. For organic matrix composites, the decomposition temperature is low, and when a critical combination of surface temperature and decomposition rate has been reached, flashover occurs, with combustion of volatiles. At the same time, heat is conducted inward from the hot face, and a region of material decomposing progresses through the thickness producing further decomposition products, which demonstrate obviously that the organic matrix composites cannot be used in high-temperature environment. Materials with outstanding thermo-mechanical and thermo-chemical properties are required for future high-temperature components, such as hypersonic space vehicle re-entry, combustion chamber of engine and rocket nozzles, in which the metal material cannot meet the requirements. However, ceramic matrix composite is one of these advanced materials, as a result of their low density, excellent resistance to ablation as well as cost effective production [11–13]. Current operating temperature in various applications are shown in Fig. 1 together with the melting temperatures of selected materials [14].

Silicon carbide matrix composite reinforced by continuous carbon fibers (C/SiC) is a kind of great potential high-temperature structural material in aeronautics and astronautics with low specific weight, high specific strength, high specific modulus, good thermal stability, oxidation resistance and excellent resistance to ablation [15]; it has better oxidation resistance than C/C and better high-temperature performance than SiC/SiC. For instantaneous lifetime (tens of seconds to several hundred seconds) of solid rocket engine, the operating temperature of C/SiC can reach 2800–3000 °C; for finite lifetime (tens of minutes to dozens of hours) of liquid rocket engine, the operating temperature of C/SiC can reach 2000–2200 °C; for long lifetime (hundreds of hours to thousands of hours) aircraft engine, the operating temperature of C/SiC is 1650 °C.

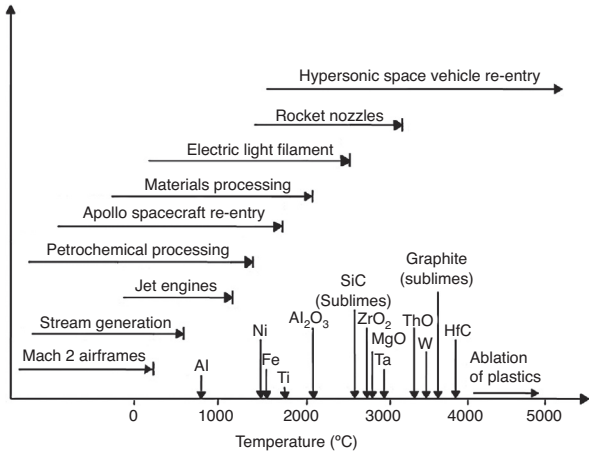

Fig. 1 – Typical operating temperatures in high-temperature environments [14].

The evolution of the morphology and microstructure of C/SiC composites during ablation is required to evaluate the aerodynamic configuration of the components and the service life of the ablation resistance. The common texting methods are oxyacetylene flame ablation, plasma arc ablation, and kerosene–liquid oxygen flame ablation. Oxyacetylene flame ablation method is the simplest and easiest to conduct with the lowest cost. Oxyacetylene flame testing was often used to simulate the rocket engine exhaust flame [16]. Chen et al. [17–21] had studied the morphology and microstructure of C/SiC composites ablated by oxyacetylene at different temperatures. Fang et al. [22] had compared the ablation property of C/SiC composites in dry air and air mixed with water vapor.

C/C composites are limited in their industrial applications due to their high sensitivity to oxidative environments which are oxidizable above 400–500 °C. However, C/SiC composites can be used in high-temperature oxidation environment, which has excellent resistance ablation performance. In high-temperature environment, SiC matrix surface would produce a highly viscous melt SiO_2 layer, which would cover the burned surface, working as an anti-oxidizing protective barrier. The melt layer also continues to adsorb a significant amount of heat by virtue of endothermic processes and due to the phase transitions of silica [23]. In the last several years, SiC doped carbon/carbon (C/C) composites for the purpose of improving the oxidation/ablation resistance had been largely reported. Among these works, various methods had been attempted including precursor infiltrations and pyrolysis (PIP) [24], chemical vapor infiltration (CVI) [25], slurry infiltration [26,27], reactive melt infiltration (RMI) [28–31] and so on. Furthermore, ablation behaviors at ultra-high temperature of doping with refractory metal compounds (such as ZrC, HfC, TaC, ZrB_2) also attracted attention increasingly [32–36].

In this paper, different ablation properties and microstructures of C/SiC composites were reviewed thoroughly; in the meantime, the ablation mechanisms were summarized and ablation physical models were also put forward.

Table 1 – Comparison of the ablation property of C/SiC composites under different situations.

No.	Fabrication	Density (g/cm^3)	Open porosity (%)	T (°C)	t (s)	Gas press (MPa)		Gas flux (L/h)		Linear ablation rate (mm/s)	Mass ablation rate ($mg\,s^{-1}$)	Ref.
						O_2	C_2H_2	O_2	C_2H_2			
1	PIP	2.00	4.4	2900	180	0.1	0.5	1656	1296	0.0025	–	[18]
2	PIP	1.93	<11	2100	30	0.4	0.095	1512	1116	0.0622	42.5	[24]
				2050		0.4	0.095	800	400	0.0466	8.7	
3	PIP	1.95	9	3000	80	0.4	0.095	1512	1116	0.061	7.16	[36]
4	CVI	–	–	1760/1740	600	0.45	0.09	248	148	–	2.05/0.55	[22]
5	CVI	2.37	10	>3000	–	0.4	0.095	1512	1116	0.083	–	[40]
6	CVI	2.00	12	–	20	0.4	0.095	1512	1116	0.042	10.3	[41]
		2.87	2.80							0.005	17.3	
7	LSI	2.41	0.92	3100	20	–		–		0.003	11.3	[42]
		2.12	0.81							0.002	7.3	

2. Ablation property and macromorphology of C/SiC composites

The ablation property and morphology of the C/SiC composites depend upon the mass transfer process, which are generally associated with complex thermal physico-chemical changes, heat-mass transfer processes and irreversible changes of thermo-mechanical and thermo-physical properties. Table 1 has listed the different ablation property of C/SiC composites under different situations. It can be seen that the ablation rates on the list were with obvious difference. The linear ablation rates of No. 7 samples in Table 1 were strikingly lower than the others, which might be the cause of the lowest open porosity. At the same time, the linear ablation rate decreased with decreasing open porosity obviously. Doubtlessly, the lower the porosity, the less the channels of thermal oxidizing components went into the interior of matrix. So, the ablation could only occur at the surface of the material, which reduced the linear ablation rate. However, due to the different doping carbon content in the No. 7 samples, it led to the decrease of density and porosity. Fig. 2 has shown the relationship between density and linear ablation rate of

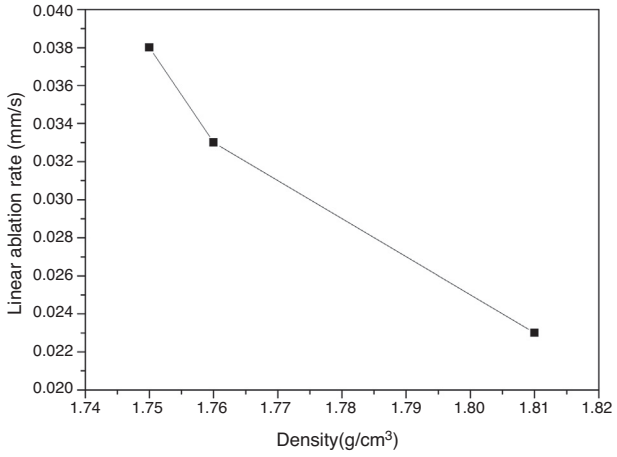

Fig. 2 – Relationship between density and linear ablation rate of C/SiC composites [37].

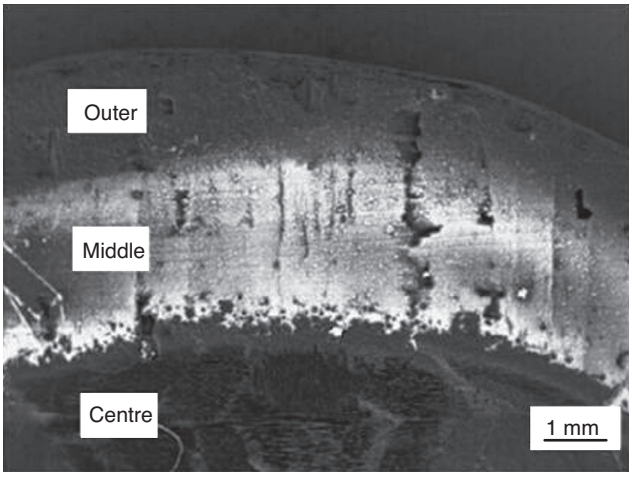

Fig. 3 – SEM photograph of the as-ablated C/SiC composites [20].

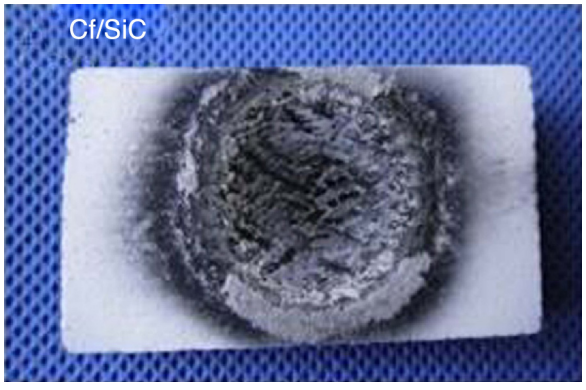

Fig. 4 – Photograph of the obtained C/SiC composites [36].

C/SiC composites [37]. It pointed out that the linear ablation rate decreased with increasing density of C/SiC composites.

Fang et al. [20] showed the ablated surface of C/SiC composites prepared by LPCVI, which could be divided into three regions from center to external after oxyacetylene torch testing (Fig. 3). Yan et al. [36] also reported this discovery as shown in Fig. 4. Three obvious regions were shown after

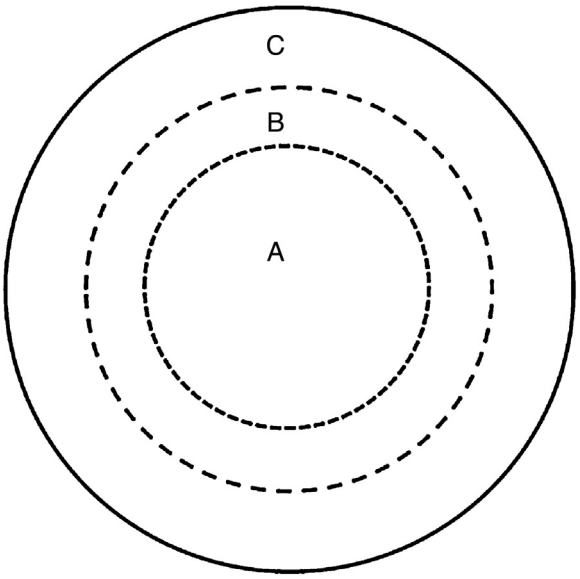

Fig. 5 – Schematic drawings of the ablated surface of the obtained composites.

80 oxyacetylene torch testing. Fig. 5 is the schematic drawings of the ablated surface of the obtained C/SiC composites, were A represented center ablation region, B represented transition erosion region and C represented border oxidation region. As shown in Fig. 4, a big pit (denoted as zone A in Fig. 5) without covering of any oxide layer appeared in the center of the C/SiC composite. A circle of glass-like layer covered the edge of the ablated pit despite falling off of some parts (denoted as zone B in Fig. 5); while the outer region with covering of frost-like oxide products remains nearly untouched (denoted as zone C in Fig. 5). It was reported the linear and mass ablation rates were 0.061 ± 0.003 mm/s and 1.46 ± 0.05 mg/cm^2 s, respectively after oxyacetylene torch testing [36]. However, Chen et al. [18] had shown that the linear ablation rate of the center region was only 0.0025 mm/s, which was the No.1 in Table 1 and the center ablation region was covered by turbostratic carbon (TC) as shown in Fig. 6. That was because the excess of the acetylene over oxygen in the premixed gases produced reduced flames, which led to the pyrolysis of the acetylene to hydrogen and free carbon. Acetylene obeyed the following pyrolysis reaction [38,39]:

$$C_2H_2(g) = 2C(s) + H_2(g) \quad (1)$$

The free carbon particles moved along the high-velocity combustion oxyacetylene gas diffusing into the body of the sample and deposited on the surface of the center ablation region to form TC coating (Fig. 6(b)). So, the linear ablation rate is significantly lower than the linear ablation rate. This phenomenon was also reported by Yan et al. [36]. Moreover, the morphology of the composites was still divided into three regions after ablation (Fig. 6(a)).

In addition, some coatings, such as ZrC and SiC, would greatly improve the ablation resistance of C/SiC composites [40,41]. Wu et al. [40] had studied the ZrC coating prepared on the surface of SiC-coated C/C composites to improve ablation resistance of SiC-coated C/C composites. After ablation for 30 s in oxyacetylene flame, the linear ablation rate was only 0.9×10^{-3} mm/s, and the weight was increased by 2.0×10^{-3} g/s. The excellent ablation resistance was mainly attributed to the formation of a dense and continuous ZrO_2 layer from the oxidation of the ZrC coating working as thermal barrier, and thus reducing the diffusion of oxygen.

In the oxyacetylene condition, ablation of the coating generally consists of three parts. They were thermo-mechanical, thermo-chemical, and thermo-physical processes resulting from high temperature, pressure, and velocity of combustion flame. During the ablation process, the reactions $ZrC + O_2 \rightarrow ZrO_2 + CO/CO_2$ would occur and produce ZrO_2, which increased the weight of specimen and formed a liquid ZrO_2 layer in the ablation central region. The liquid ZrO_2 layer acted as a thermal barrier and reduced the diffusion of oxygen. However, the partial ZrO_2 layer in the ablation central region could be carried away by the combustion flame with high velocity, following the drop of thickness of the coating.

To sum up, the ablated surface of C/SiC composites can be divided into three regions from center to external, i.e. center ablation region, transition erosion region and border oxidation region. Table 1 illustrates the different linear ablation rates and mass ablation rates of the C/SiC composites with the preparation methods, the density and open porosity, the ablation temperature, ablation time and the gaseous flow. As shown

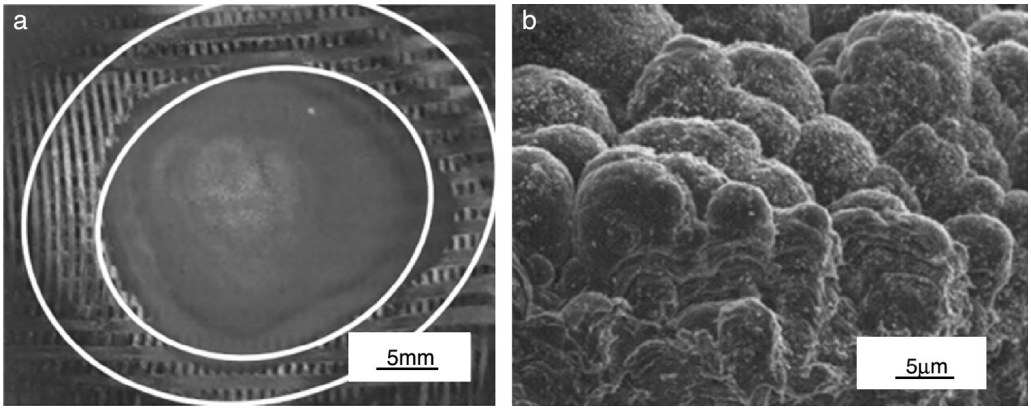

Fig. 6 – (a) Photograph of the as-ablated sample; (b) scanning electron micrographs of turbostratic carbon (TC) in the center ablation region [18].

Table 2 – Reactions might take place in different regions [26,42,43].

Sublimation and oxidation of carbon	
$C(s) = C(g)$ (273-3823 K)	(2)
$2C(s) + O_2(g) = 2CO(g)$ (273–3300 K)	(3)
$C(s) + O_2(g) = CO_2(g)$ (273–3300 K)	(4)
$4C(s) + O_2(g) = 2C_2O(g)$ (273–3300 K)	(5)
$C(s) + O_2(g) = C_3O_2(g)$ (273–3300 K)	(6)
$C(s) + H_2O(l) = CO(g) + H_2(g)$ (273–373 K) $C(s) + H_2O(g) = CO(g) + H_2(g)$ (373–3300 K)	(7)
Sublimation, oxidation and catalytic oxidation of silicon carbide	
$SiC(s) = SiC(g)$ (273–3300 K)	(8)
$SiC(g) = Si(g) + C(s)$ (3103–3300 K)	(9)
$SiC(g) + C(s) = SiC_2(g)$ (3103–3300 K)	(10)
$SiC(g) + Si(g) = Si_2C(g)$ (3103–3300 K)	(11)
$2/3SiC(s) + O_2(g) = 2/3SiO_2(s) + 2/3CO(g)$ (273–1996 K) $2/3SiC(s) + O_2(g) = 2/3SiO_2(l) + 2/3CO(g)$ (1996–2503 K) $2/3SiC(l) + O_2(g) = 2/3SiO_2(g) + 2/3CO(g)$ (3103–3300 K)	(12)
$1/2SiC(s) + O_2(g) = 1/2SiO_2(s) + 1/2CO_2(g)$ (273–1996 K) $1/2SiC(s) + O_2(g) = 1/2SiO_2(l) + 1/2CO_2(g)$ (1996–2503 K) $1/2SiC(l) + O_2(g) = 1/2SiO_2(g) + 1/2CO_2(g)$ (3103–3300 K)	(13)
$SiC(s) + O_2(g) = SiO(g) + CO(g)$ (273–3300 K)	(14)
$2/3SiC(s) + O_2(g) = 2/3SiO(g) + CO_2(g)$ (273–3300 K)	(15)
$2/3SiC(s) + O_2(g) = 1/3Si_2O_2(g) + 2/3CO_2(g)$ (273–3300 K)	(16)
$SiC(s) + O_2(g) = 1/2Si_2O_2(g) + CO(g)$ (273–3300 K)	(17)
Sublimation and catalytic oxidation of silicon dioxide	
$SiO_2(l) = SiO_2(g)$ (1996–3300 K)	(18)
$1/3SiO_2(l) + C(s) = 2/3SiC(s) + CO(g)$ (1996–2503 K) $1/3SiO_2(g) + C(s) = 2/3SiC(s) + CO(g)$ (2503–3103 K) $1/3SiO_2(g) + C(s) = 2/3SiC(l) + CO(g)$ (3103–3300 K)	(19)
$1/2SiO_2(l) + C(s) = 1/2SiC(s) + 1/2CO_2(g)$ (1996–2503 K) $1/2SiO_2(g) + C(s) = 1/2SiC(s) + 1/2CO_2(g)$ (2503–3103 K) $1/2SiO_2(g) + C(s) = 1/2SiC(l) + 1/2CO_2(g)$ (3103–3300 K)	(20)
$SiO_2(l) + CO(g) = SiO(g) + CO_2(g)$ (1996–3300 K)	(21)
$2SiO_2(l) + SiC(s) = 3SiO(g) + CO(g)$ (1996–3103 K) $2SiO_2(l) + SiC(l) = 3SiO(g) + CO(g)$ (3103–3300 K)	(22)
Sublimation and oxidation of silicon	
$Si(s) = Si(g)$ (1687–3300 K)	(23)
$Si(s) + O_2(g) = SiO_2(s)$ (273–1996 K)	(24)
(24) $2Si(g) + O_2(g) = 2SiO(g)$ (3173–3300 K)	(25)
$Si(g) + SiO_2(l) = 2SiO(g)$ (1996–3300 K)	(26)

in Table 1, the higher the density, the lower the ablation rate; the lower the ablation temperature and less time, the lower the ablation rate, and the ablation rate of C/SiC composites by oxyacetylene torch under abundant oxygen environment was higher obviously than that under free oxygen environment.

3. Microstructure and ablation mechanism of SiC matrix

As a result of the different temperature and pressure at different ablation regions, the microstructure and ablation

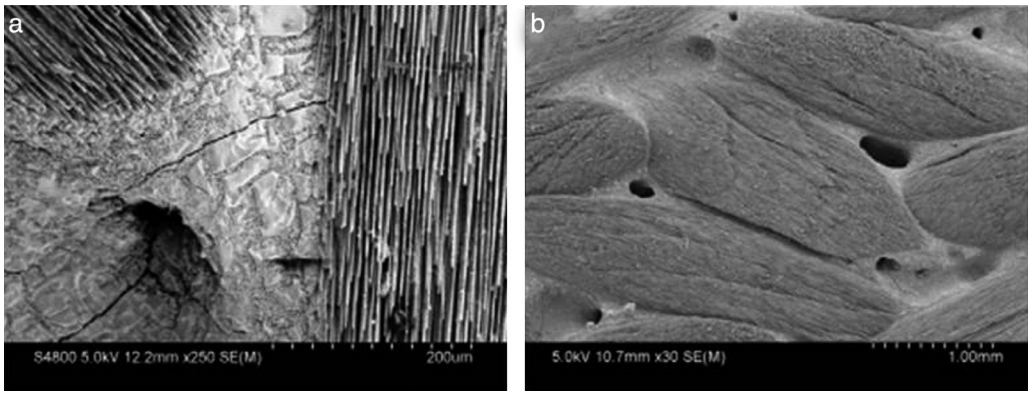

Fig. 7 – SEM morphologies of the surface areas for the ablated C/SiC composite: (a and b) the ablated pit areas in the center region [36].

mechanism of SiC matrix will have big differences. In the meantime, the ablation morphologies are also changed with the change of preparation methods and the gas flow, etc. The chemical reactions are extremely complex in the process of ablation. All of the following reactions possibly proceeded in Table 2 under the oxyacetylene flame temperature [26,42,43].

In the center ablation region, ablation is the severest, due to the highest temperature and pressure. Fig. 7 shows the microstructures of the surface areas for the ablated C/SiC composites in the center region. For Fig. 7(a), only bare fiber bundles and the exposed pores existed, and there were no oxide layers covering the surface of the pit. Moreover, microcracks were produced due to the severe thermal shock during testing. Some micropores could be seen in Fig. 7(b), and the formation mechanism of these micropores was a combinative effect containing the expansion of gases inside the closed pores and the high-speed oxyacetylene torch [19]. Since oxyacetylene torch armed at center ablation region, material surface had the highest temperature (above 3000 °C), and SiC was in a state of sublimation (the sublimation of SiC temperature is 2700 °C (Eq. (8)). At the beginning, first, part of SiC matrix was sublimated. With the start of active oxidation of SiC, some SiO gas was formed directly instead of protective SiO_2 (Eqs. (14), (15), and (22)), and the formed silica was also taken away under the high-speed flow scouring. In addition, since vapor pressure of SiO_2 was about 7 kPa at 1900 °C [44], the liquid SiO_2 transferred to gaseous product during the process of ablation [45]. The flowing gas above sample surface renovated quickly under high-speed ablation gases; therefore, liquid SiO_2 could not fill the holes and the naked fibers were found. So, in the center region, the main ablation behavior was sublimation of SiC and thermal physical evaporation of SiO_2. Although a thermo-chemical reaction was one of the ablation reactions in ablation center region, thermo-physical and thermo-mechanical reactions by flame seemed to be more important during ablation process [46].

If the ablation condition is changed, the microstructure of the ablated composites will have a big difference. Wei et al. [24] had compared the ablation behavior of C/SiC composites by oxyacetylene torch under oxygen free environment and abundant oxygen environment. Fig. 8 was ablation morphology of center region under abundant oxygen environment. It had a

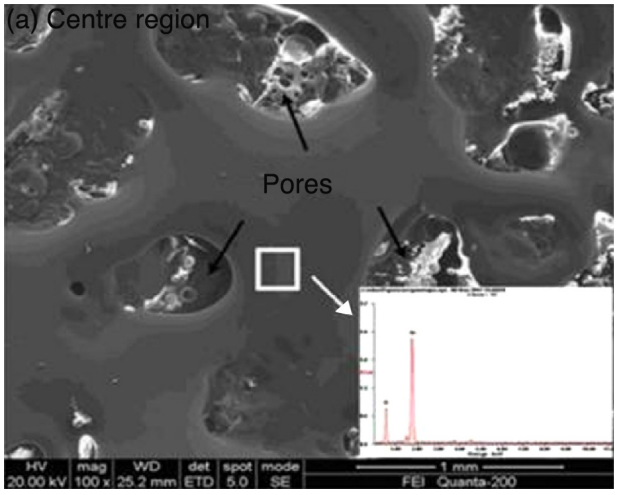

Fig. 8 – Ablation morphology of center region under abundant oxygen environment [24].

big difference from the above phenomenon because the oxygen was sufficient in the process of ablation, and the ablation parameters could be seen in Table 1 No. 2. The surface was covered by SiO_2 film with no bare fiber discovered. Pores were also observed on the surface of film. Due to the abundant oxygen environment, SiC matrix was oxidized to SiO_2. SiO_2 could sequentially react to form a gas (Eqs. (21) and (22)) and also directly gasify (SiO_2 boiling point 2230 °C) (Eq. (18)). During the ablation procedure, the formation of the oxide layer was a dynamic equilibrium process [41]. On the one hand, the oxide covering the surface was blown away by the high-velocity gas, and on the other hand, the new oxide would be formed by the oxidation of the inner matrix. In this region, the generation rate of oxide was higher than the denudation rate. Then the surface of the composites was completely covered by SiO_2 with pores. So, under abundant oxygen environment, ablation mechanisms mainly were oxidation erosion in center ablation region [24].

Fan et al. [41] had shown ablation morphology of transition region and border oxidation region after ablation as shown in Fig. 9. This result was similar to Fang et al. [20] reported

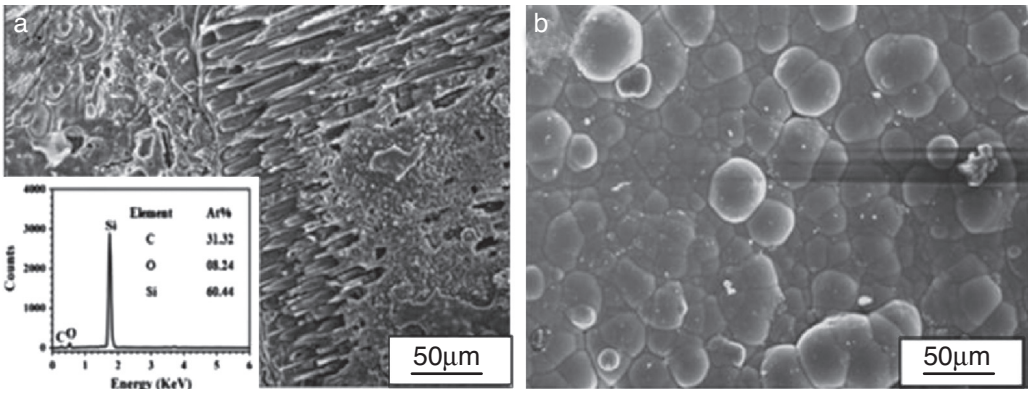

Fig. 9 – Ablation morphologies of C/SiC composites prepared by CVI: (a) the transition region and (b) the border oxidation region after ablation [41].

before. In the transition region, oxyacetylene torch testing annealed at comparatively lower temperature and pressure than center ablation region and led to the mild oxidation. For Fig. 9(a), the scour traces was obvious on the surface owing to the mechanical erosion. Parts of SiC were oxidized forming SiO_2 layer, which occurred in the reactions (12) and (13). The SiO_2 not only protected the inter-bundle pores on the erosion surface from further attack by the thermal oxidizing atmosphere, but also acted as a barrier to oxygen diffusion due to its low oxygen permeability, leading to the homogeneous erosion [26]. Fig. 9(b) was the border oxidation region, which was the farthest from the ablation center. In this region, the ablation degree was the lightest. The cellular structure of initial SiC coating was clearly seen, and some white and spherical SiO_2 particles formed rice-like shapes on the surface of the aggregates of SiC. The SiO_2 particles were generated from the oxidation of Si and SiO steam that was blown away by the oxyacetylene flame from the center region in accordance with reactions (9), (14), (21) and (22). When Si and SiO steam was oxidized, high-melting-point silica would be absorbed by the outer region, which had a relatively low temperature. According to the gas dynamics [47], the condensation of the vapor would occur when the supersaturation degree reached the critical values. The relation between supersaturation and nucleus size obeys the Gibbs–Thomson law [48]:

$$B = \frac{1}{\left[\ln\left(\frac{1}{\lambda\mu}\right)\right]} \tag{27}$$

Eq. (27) predicts that as the supersaturation of reactant μ increases, the nucleus size B increases exponentially. As analyzed above, thermo-mechanical attacks and thermo-chemical reactions are the ablation mechanism in transition region, however, thermo-chemical reaction is the only ablation mechanism in border oxidation region.

However, the microstructures of the ablated composites were different with the change of preparation methods. Yan et al. [19] had reported other ablation morphologies of three-dimensional orthogonal C/SiC composites in transition region and border oxidation region as shown in Fig. 10, which was significantly different from the above discussed. It was because the preparation methods of C/SiC composites were different. It could be seen from Fig. 10(a) that the surface SiC matrix was cataclastic shapes with a particle size less than 10 μm. Parts of SiC particles were oxidized into the SiO_2. It was attributed to the mechanical erosion by high speed oxyacetylene torch to smash the SiC particles in a short time [19]. Fig. 10(b) shows SEM micrographs of the border oxidation region. The surface of this region contained three zones, e.g., zone I where the fibers were perpendicular to the surface, zone II where fibers were parallel to the surface and zone III where there was SiC

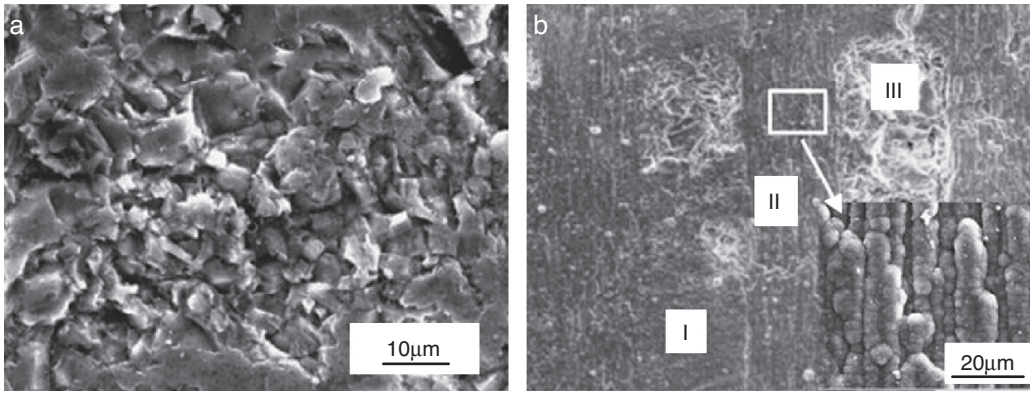

Fig. 10 – Ablation morphologies of C/SiC composites prepared by PIP: (a) the transition region and (b) the border oxidation region after ablation [19].

Table 3 – The linear expansion coefficient of silicon carbide [44,52].

Temperature (K)	293	373	473	573	673	773	873
Linear expansion coefficient $\alpha \times 10^{-6}$ (K)	3.5	3.7	4.1	4.4	4.6	4.9	5.1
Temperature (K)	973	1073	1273	1473	1673	1873	2073
Linear expansion coefficient $\alpha \times 10^{-6}$ (K)	5.3	5.6	5.8	6.1	6.2	6.4	6.5

coating. In zone I, the surface was covered uniformly by spherical SiC grains. In zone II, SiC particles agglomerated to form a strip structure along the fiber direction, and the strips were nearly 5–10 μm wide and 100 μm long (Fig. 10(b)). Because of poor wettability between SiC and carbon fibers, recrystallized SiC strips-like were formed [19]. Zone III was SiC matrix among carbon fiber yarns. Non-compactness of SiC matrix in this zone caused pits with size close to $260 \times 670\ \mu m^2$. The white stuff was SiO_2 oxidized from SiC. So, in transition ablation region, ablation mechanisms mainly are oxidation and erosion mechanism, while in the border ablation region, light oxidation and recrystallization of surface SiC are the main erosion mechanisms.

The reason for the different ablation behavior of C/SiC composites prepared by CVI and PIP was because the SiC matrix microstructures were different with the different preparation methods. From Fig. 9, the deposit prepared by CVI was composed of a large number of spherical particles with a cloud-cluster shape. Among these particles, aggregation and fusion were also observed. While after the process of PIP, the microstructures of the ablated composites were totally different, as shown in Fig. 10. The SiC particles were unordered and had cataclastic shapes, which were typical matrix morphology after precursor infiltration and pyrolysis process. If the density is the same, the microstructure was different obviously, but the ablation behavior included linear ablation rate and mass ablation rate that were almost similar, which could be analyzed in Table 1.

Fig. 11 has shown some cracks on the surface of the SiC matrix in the border oxidation region [18]. The formation mechanism of the surface cracks was the CET (coefficient of thermal expansion) mismatch (perpendicular to the fiber direction) between the SiC matrix and the carbon fibers

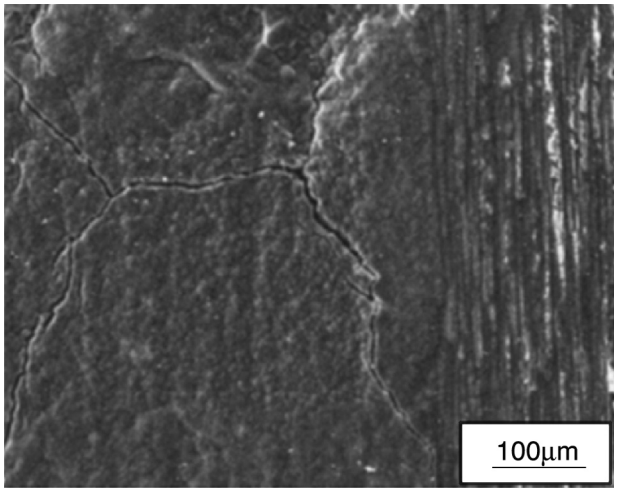

Fig. 11 – SEM morphologies of some cracks in the border oxidation region [18].

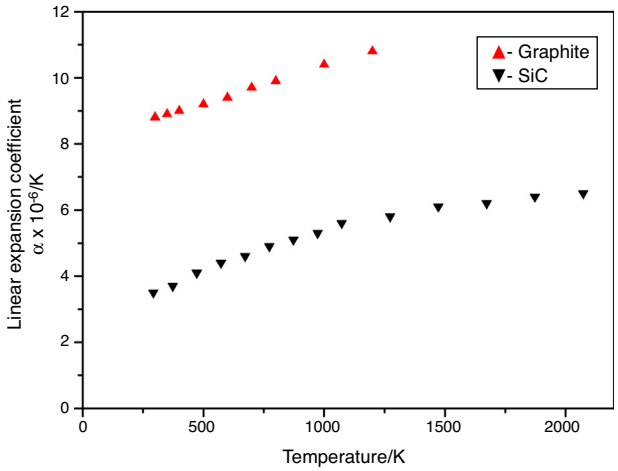

Fig. 12 – The linear expansion coefficient of graphite and SiC changing with the temperature.

[49–51]. Linear expansion coefficients of silicon carbide and graphite are displayed in Tables 3 and 4, respectively [44,52]. Fig. 12 intuitively illustrated both of the linear expansion coefficients changing with the temperature. It showed that the CTE of graphite (α_c) was larger than that of silicon carbide (α_s), which led to residual stress perpendicular to the fiber directions in the process of heating and cooling. According to Gouadec et al. [53], the residual stress (σ) can be estimated by the following formula:

$$\sigma = (\alpha_m - \alpha_f)(\Delta T)\frac{E_m E_f}{E_m + E_f} \tag{28}$$

where α_m and α_f are the CTE of SiC matrix and C fiber in the perpendicular fiber direction, ΔT is the difference between the processing temperature and the room temperature, and E_m and E_f are the Young's moduli of SiC matrix and C fiber, respectively.

In Fig. 11, both sides of the crack were SiO_2, which indicated that thermal oxygen had invaded into the cracks and induced the oxidation of the matrix. SiC matrix was oxidized forming SiO_2 with little volume expansion [19]. It was beneficial for improving the matching of the thermal expansion coefficient between matrix and fibers or for reducing the porosity and is beneficial for oxidation inhibition [18].

4. Microstructure and ablation mechanism of C fibers

As shown in Fig. 13(a), the fibers were severely corroded into needle shape, and there was no matrix remaining among fibers in the center ablation region, which indicated that the C fiber ablation behavior was different with oxidation

Table 4 – The linear expansion coefficient of graphite [44,52].

Temperature (K)	300	350	400	500	600
Linear expansion coefficient $\alpha \times 10^{-6}$ (K)	8.8	8.9	9.0	9.2	9.4
Temperature (K)	700	800	1000	1200	–
Linear expansion coefficient $\alpha \times 10^{-6}$ (K)	9.7	9.9	10.4	10.8	–

behavior significantly [24]. Chen et al. [17] had also observed the naked fibers formed in ablation center. During the ablation process, the end parts of the carbon fibers were tapered [54]. During the oxidation process, the end parts of the carbon fibers were flat-bottomed [55,56]. In general, ablation phenomenon of C fibers is a combination of oxidation and erosion factors from high temperature, pressure, and velocity of oxyacetylene flame. Fan et al. [41] had reported two kinds of carbon fibers with different shapes existing in the center region after ablation. Some carbon fibers were oxidized to a needled-liked shape, while the other carbon fibers were directly sheared by the flame presenting a flat fracture surface. However, in the transition region, SiC matrix was not sublimated completely and still some SiC existed in the samples which coated the C fiber as shown in Fig. 13(b). The white material coated matrix was SiO_2, which was formed according to reactions (12) and (13). Due to the protection of SiC matrix and SiO_2 layer, C fiber did not receive serious thermo-mechanical attack.

For Fig. 13, the SiC matrix had decomposed completely. On the one hand, the latent heat of SiC sublimation is 19.825 MJ/kg, while the C fiber is 59.75 MJ/kg, which is three times of the latent heat of SiC sublimation [57,58], and on the other hand, the sublimation temperature of SiC matrix is 2700 °C, while that of carbon fiber is 3550 °C which is higher than that of SiC [59]. Therefore, C fiber is in the state of incomplete sublimation. Due to the above factors, the ablation rate of SiC matrix is faster than that of C fiber under the ablation circumstance, leading to C fiber having better ablation resistance than SiC matrix. Liu et al. [60] had reported a similar result that the erosion speed of SiC addition in C/C composites was faster than that of pyrocarbon when heat fluxes exceeded a certain value under oxyacetylene torch. Liu et al. [61] also reported that the oxidation of SiC particles was prior to the oxidation of carbon during the ablation. Although carbon has a lower initial temperature of oxidation than SiC in the view of chemical thermodynamics, the oxidation of the composites during ablation is determined by the rates of reactions (2)–(17) as the surface temperature rose rapidly to higher than 1700 °C. In this case, in the center region, the ablation mechanisms of C fibers mainly are thermo-physical and thermo-mechanical erosion.

Due to the different ablation conditions, the microstructures of C fibers were different. Yan et al. [19] reported the morphologies of C fibers in ablation transition region as shown in Fig. 14. Fig. 14(a) shows that the carbon fibers were perpendicular to the surface in transition region. Due to its poorer oxidation resistance than SiC, the carbon fibers perpendicular to the surface of ablation were eroded, forming the depression structure comparing with the matrix. In Fig. 14(b), the carbon fibers were parallel to the surface in outer ablation region and the fibers were oxidized into several parts. The lower temperature led to the mild oxidation in this region and the CTE mismatch between the fibers and the SiC matrix led to the fracture of fibers. So, the thermo-chemical erosion is the main ablation mechanism of C fibers in the transition region.

5. Ablation physical model

Fig. 15 is the ablation physical model at the ablation center. Fig. 15(a) is the structure drawing of C/SiC composites before ablation. For the high thermal conductivity of carbon fibers, heat quantity in the front of the fibers quickly transferred down the longitudinal direction of the carbon fibers [52,62], in addition, the SiC matrix ablation rate was greater than that of C fiber in this region, resulting in C fiber constantly exposed to the thermal erosion environment. In the ablation process, the interface between C fiber and SiC matrix would form vortex, as shown in Fig. 15(b), where the heat would be gathered, which speeded up the ablation process. As time goes, the front of C fiber exposed to thermal erosion environment lasted longer than that in the end, leading to the front of C fiber becoming more and more sharp, and the end was relatively coarse.

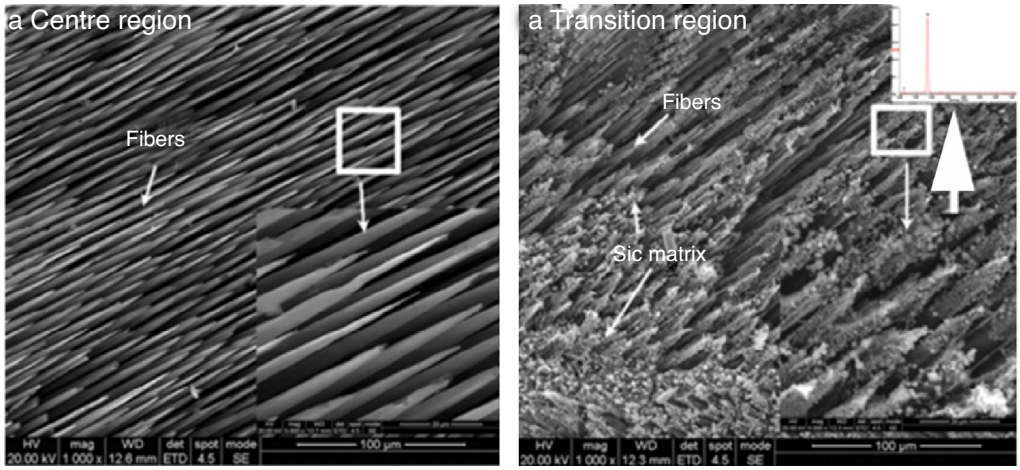

Fig. 13 – Morphologies of C/SiC composites: (a) center region and (b) transition region after ablation [24].

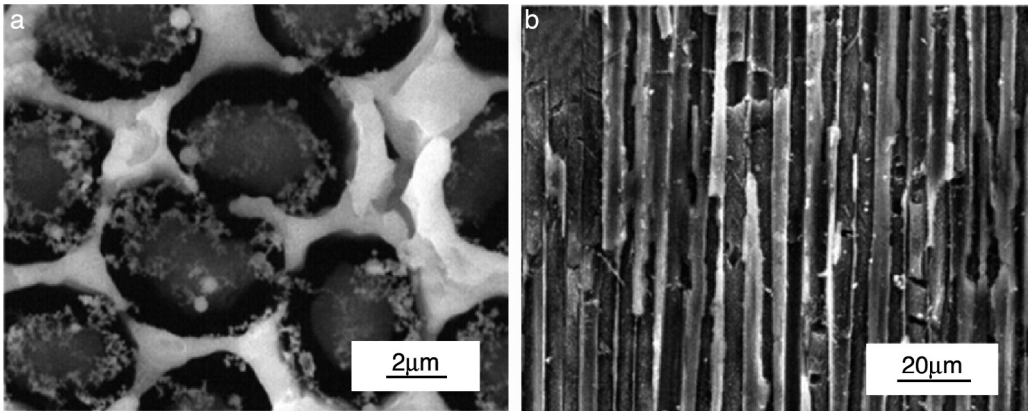

Fig. 14 – Morphologies of transition region: (a) fibers were perpendicular to the surface and (b) fibers were parallel to the surface [19].

Because of the high thermal conductivity of carbon fiber and the difference of the sublimation velocity in adjacent ends, a needle-like microstructure was formed. Sublimating ablation, a kind of thermo-physical attack, was the main ablation behavior in the center region.

As discussed above, for C/SiC composites, the ablation under oxyacetylene torch should be a complex process, which mainly consisted of oxidation, evaporation, mechanical erosion and perhaps some thermal decomposition. In fact, the thermal decomposition of SiC and evaporation of SiO_2 continue to adsorb a significant amount of heat by virtue of endothermic processes. Although the ablation morphologies are different with the different preparation methods, the ablation mechanisms are almost the same. The ablation schematic diagram of C/SiC composites is shown in Fig. 16. It can be seen that there are three ablation regions ("I", "II" and "III") and the heat flow direction is from center region to outside region, which leads to the temperature of center region being highest and the border oxidation region being lowest. In the center region "I", SiC matrix sublimit completely, presenting as bare needle shape C fibers, which shows the process of ablation in Fig. 15. In the transition region "II", SiC matrix is oxidized to SiO_2 film. The oxide layer attaches on the matrix, which prevents oxygen from contacting the inner materials directly [63]. In the border oxidation region "III", Si and SiO steam is oxidized to SiO_2, which comes from the center region. After the consumption of SiC matrix, C fibers start to be oxidized to CO and CO_2. As a result, all the gaseous products resulting from oxidation and high temperature lead to high mass loss rate and linear recession rate [64]. Based on the above analyses, it can be found that the main ablation mechanism in "I" region is thermo-physical and thermo-mechanical attacks, while in "II" and "III" thermo-chemical reactions, it is more important during ablation.

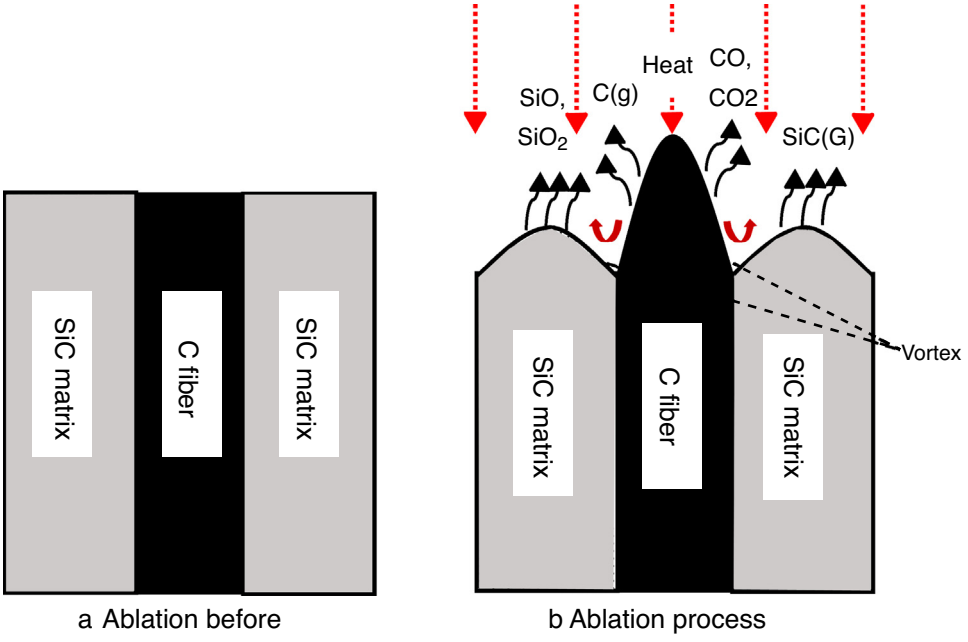

Fig. 15 – Ablation physical model at the ablation center.

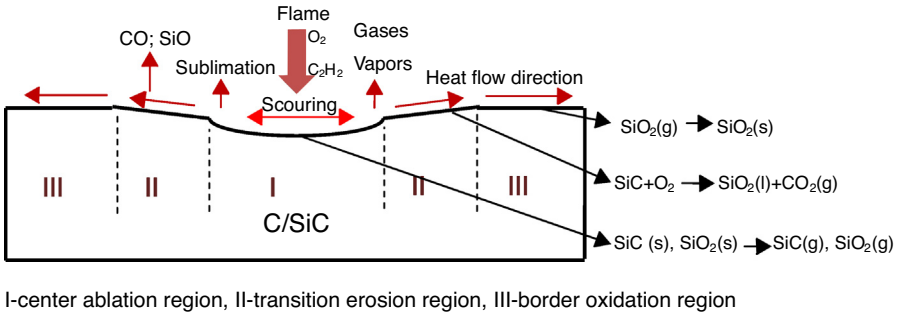

Fig. 16 – Ablation schematic diagram of C/SiC composites.

6. Conclusion

In this paper, different ablation properties of C/SiC composites were compared thoroughly, in addition the ablation mechanisms were summarized adequately. The conclusions can be drawn as follows.

(1) The ablated surface of C/SiC composites can be divided into three regions from center to external after oxyacetylene torch testing.
(2) In general, the higher the density, the lower the ablation rate; the lower the ablation temperature and less time, the lower the ablation rate, and that the preparation methods also have a great influence on the ablation property.
(3) Thermo-physical and thermo-mechanical attacks are the main ablation behavior in the center region; oxidation is the main ablation behavior in the transition region and the border oxidation region. However, under abundant oxygen environment, ablation mechanisms mainly are oxidation erosion.
(4) A needle-like microstructure was formed, because of the high thermal conductivity of carbon fiber and the difference of the sublimation velocity in adjacency ends.

Conflict of interest

The authors declare no conflicts of interest.

Acknowledgements

The present work was supported by the Funding of Jiangsu Innovation Program for Graduate Education (the Fundamental Research Funds for the Central Universities), KYLX15_0308, and a Project Funded by the Priority Academic Program Development of Jiangsu Higher Education Institutions.

REFERENCES

[1] Gibson AG, Otheguy TME, Browne TNA, Feih S, Mouritz AP. High temperature and fire behaviour of continuous glass fibre/polypropylene laminates. Composites A 2010;41:1219–31.
[2] Gibson AG, Wu YS, Evans JT, Mouritz AP. Laminate theory analysis of composites under load in fire. J Compos Mater 2006;40:639–58.
[3] Gibson AG, Wright PNH, Wu Y-S, Mouritz AP, Mathys Z, Gardiner CP. The integrity of polymer composites during and after fire. J Compos Mater 2004;38:1283–308.
[4] Mouritz AP, Feih S, Kandare E, Mathys Z, Gibson AG, Jardin PED, et al. Review of fire structural modelling of polymer composites. Composites A 2009;40:1800–14.
[5] Bai Y, Valleé T, Keller T. Modeling of thermal response for FRP composites under elevated and high temperatures. Compos Sci Technol 2008;68(1):47–56.
[6] Bai Y, Keller T. Modeling of stiffness of FRP composites under elevated and high temperatures. Compos Sci Technol 2008;68:15–6, 3099–3106.
[7] Gibson AG, Browne TNA, Feih S, Mouritz AP. Modeling composite high temperature behavior and fire response under load. J Compos Mater 2012;46:2005–22.
[8] Lattimer BY, Ouellette J. Properties of composite materials for thermal analysis involving fires. Composites A 2006;37:1068–81.
[9] Feih S, Mathys Z, Gibson AG, Mouritz AP. Modelling the tension and compression strengths of polymer laminates in fire. Compos Sci Technol 2007;67:551–64.
[10] Easby RC, Feih S, Konstantis C, Delfa GL, Miano VU, Elmughrabi A, et al. Failure model for phenolic and polyester pultrusions under load in fire. Plastics Rubber Compos 2007;36:379–88.
[11] Khan MB. An investigation of the ablation behavior of advanced ultrahigh-temperature EPDM/epoxy insulation composites. Polym Plast Technol Eng 1996;35:187–206.
[12] Beyer S, Schmidt S, Peres P, Bouchez M. Advanced ceramic matrix composite materials for current and future propulsion system applications. In: 41st AIAA/ASME/SAE/ASEE joint propulsion conference & exhibit. 2005.
[13] Mital SK, Murthy PLN. Characterizing the properties of a C/SiC composite using micromechanics analysis. In: 42nd AIAA/ASME/SAE/ASEE structures, Structure Dynamics, and materials conference & exhibit. 2001.
[14] Meetham GW. High-temperature materials—a general review. J Mater Sci 1991;26:853–60.
[15] Beyer S, Strobel F, Knabe H. Development and testing of C/SiC components for liquid rocket propulsion applications. Pap Am Inst Aeronaut Astronaut 1999;12:1–11.
[16] Song GM, Zhou Y, Wang YJ. Effect of carbide particles on the ablation properties of tungsten composites. Mater Charact 2003;50:293–303.
[17] Chen ZF, Fang D, Miao YL, Bo Y. Comparison of morphology and microstructure of ablation centre of C/SiC composites by oxy-acetylene torch at 2900 °C and 3550 °C. Corros Sci 2008;50:3378–81.

[18] Chen ZF, Yan B. Morphology and microstructure of three-dimensional orthogonal C/SiC composites ablated by an oxyacetylene flame at 2900 °C. Int J Appl Ceram Technol 2009;6:164–70.
[19] Yan B, Chen ZF, Zhu J, Zhang J, Jiang Y. Effects of ablation at different regions in three-dimensional orthogonal C/SiC composites ablated by oxyacetylene torch at 1800 °C. J Mater Process Technol 2009;209:3438–43.
[20] Fang D, Chen ZF, Song Y, Sun Z. Morphology and microstructure of 2.5 dimension C/SiC composites ablated by oxyacetylene torch. Ceram Int 2009;35:1249–53.
[21] Yan B, Chen ZF, Li C, Fang D, Zhang Y, Wang LB. Ablation morphology and microstructure of 3D orthogonal C_f/SiC composites prepared by PIP. Sci Eng Compos Mater 2008;15:71–8.
[22] Fang XF, Liu FS, Su HQ, Liu B, Feng X. Ablation of C/SiC, C/SiC–ZrO_2 and C/SiC–ZrB_2 composites in dry air and air mixed with water vapor. Ceram Int 2014;40:2985–91.
[23] Natali M, Monti M, Kenny JM, Torre L. A nanostructured ablative bulk molding compound: development and characterization. Compos Part A: Appl Sci 2011;42:1197–204.
[24] Li W, Xiang Y, Wang S, Ma Y, Chen ZH. Ablation behavior of three-dimensional braided C/SiC composites by oxyacetylene torch under different environments. Ceram Int 2013;39:463–8.
[25] Yin J, Zhang HB, Xiong X, Zuo J, Tao H, Yin J, et al. Ablation properties of C/C–SiC composites tested on an arc heater. Solid State Sci 2011;13:2055–9.
[26] Tang SF, Deng JY, Liu WC, Yang K. Mechanical and ablation properties of 2D-carbon/carbon composites pre-infiltrated with a SiC filler. Carbon 2006;44:2877–82.
[27] Tang SF, Deng JY, Wang SJ, Liu WC, Yang K. Ablation behaviors of ultra-high temperature ceramic composites. Mater Sci Eng A 2007;465:1–7.
[28] Li ZQ, Li HJ, Li W, Wang J, Zhang SY, Guo J. Preparation and ablation properties of ZrC–SiC coating for carbon/carbon composites by solid phase infiltration. Appl Surf Sci 2011;258:565–71.
[29] Li ZQ, Li HJ, Zhang SY, Wang J, Li W, Sun FJ. Effect of reaction melt infiltration temperature on the ablation properties of 2D C/C–SiC–ZrC composites. Corros Sci 2012;58:12–9.
[30] Li ZQ, Li HJ, Zhang SY, Li KZ. Microstructure and ablation behaviors of integer felt reinforced C/C–SiC–ZrC composites prepared by a two-step method. Ceram Int 2012;38:3419–25.
[31] Lee YJ, Joo HJ. Ablation characteristics of carbon fiber reinforced carbon (CFRC) composites in the presence of silicon carbide (SiC) coating. Surf Coat Technol 2004:180–1, 286–289.
[32] Shen XT, Li KZ, Li HJ, Du HJ, Cao WF, Lan FT. Microstructure and ablation properties of zirconium carbide doped carbon/carbon composites. Carbon 2010;48:344–51.
[33] Li SP, Li KZ, Li HJ, Li YL, Yuan QL. Effect of HfC on the ablative and mechanical properties of C/C composites. Mater Sci Eng A 2009;517:61–7.
[34] Chen ZK, Xiong X, Li GD, Sun W, Long Y. Texture structure and ablation behavior of TaC coating on carbon/carbon composites. Appl Surf Sci 2001;257:656–61.
[35] Corral EL, Wslker LS. Improved ablation resistance of C–C composites using zirconium diboride and boron carbide. J Eur Ceram Soc 2001;30:2357–64.
[36] Yan CL, Liu RJ, Cao YB, Zhang CG, Zhang DK. Ablation behavior and mechanism of C/ZrC, C/ZrC–SiC and C/SiC composites fabricated by polymer infiltration and pyrolysis process. Corros Sci 2014;86:131–41.
[37] Pan YS, Xu YD, Chen ZF, Cheng LF, Zhang LT, Xiong DS. Ablation properties analysis of 2D C/SiC composites. Ordnance Mater Sci Eng 2006;29:17–20.
[38] Davies RA, Scully DB. Carbon formation from aromatic hydrocarbons II. Combust Flame 1966;10:165–70.
[39] García I, Vázquez AJ. Oxy-acetylene flame chemical vapour deposition of diamond films. Part I: the influence of deposition parameters on diamond morphology. Thin Solid Films 1998;325:99–106.
[40] Wu H, Li HJ, Fu QG, Yao D-J, Wang Y-J, Ma C, et al. Microstructures and ablation resistance of ZrC coating for SiC-coated carbon/carbon composites prepared by supersonic plasma spraying. J Therm Spray Technol 2011;20:1286–91.
[41] Fan XM, Yin XW, Wang L, Cheng L, Zhang L. Processing, microstructure and ablation behavior of C/SiC–Ti_3SiC_2 composites fabricated by liquid silicon infiltration. Corros Sci 2013;74:98–105.
[42] Cui YY, Li AJ, Li B, Ma X, Bai RH, Zhang WG, et al. Microstructure and ablation mechanism of C/C–SiC composites. J Eur Ceram Soc 2014;34:171–7.
[43] Lespade P, Richet N, Goursat P. Oxidation resistance of HfB_2–SiC composites for protection of carbon-based materials. Acta Astronaut 2007;60:858–64.
[44] Liu GQ, Ma LX, Liu J. Handbook of chemistry physical properties. Beijing: Chemical Industry Press; 2002.
[45] Liu L, Li HJ, Feng W, Shi XH, Li KZ, Guo LJ. Ablation in different heat fluxes of C/C composites modified by ZrB2–ZrC and ZrB2–ZrC–SiC particles. Corros Sci 2013;74:159–67.
[46] Lee YJ, Joo HJ. Investigation on ablation behavior of CFRC composites prepared at different pressure. Compos Part A: Appl Sci 2004;35:1285–90.
[47] Emmons HW. Fundamentals of gas dynamics (section F). Princeton: Princeton University Press; 1958. p. 3.
[48] Yang Y, Zhang WG. Kinetic and microstructure of SiC deposited from $SiCl_4$–CH_4–H_2. Chin J Chem Eng 2009;17:419–26.
[49] Carrère N, Martin E, Lamon J. The influence of the interphase and associated interfaces on the deflection of matrix cracks in ceramic matrix composites. Compos Part A: Appl Sci 2000;31:1179–90.
[50] Zhang CR, Hao YK. Ceramic matrix composites. Changsha: National University of Defense Technology Press; 2001. p. 231.
[51] Kellett EA, Richards BP. The thermal expansion of graphite within the layer planes. J Nucl Mater 1964;12(2):184–92.
[52] Hicks TG, Chopey NP. Handbook of chemical engineering calculations. fourth ed. New York: McGraw-Hill; 2004.
[53] Gouadec G, Colomban P, Bansal NP. Raman study of uncoated and p-BN/SiC-coated Hi-Nicalon fiber reinforced Celsian matrix composities. In: NASA Technical Memorandum 210349; 2000.
[54] Lee YJ [Ph.D. Thesis] Effects of boron and phosphorus on the reactivity and crystallinity of diverse carbon materials. University Park, PA: Pennsylvania State University; 2001.
[55] Mei H, Cheng LF, Zhang LT, Luan XG, Zhang J. Behavior of two-dimensional C/SiC composites subjected to thermal cycling in controlled environments. Carbon 2006;44:121–7.
[56] Xiang Y, Li W, Wang S, Chen ZH. Oxidation behavior of oxidation protective coatings for PIP–C/SiC composites at 1500 °C. Ceram Int 2012;38:9–13.
[57] Aylward GH, Findlay TJV. SI Chemical Data. sixth edition ed. Milton, Queensland, Australia: John Wiley & Sons; 2007.
[58] Wang KX. Composite foundation of solid rocket engine. Beijing: Tsinghua University press; 1992. p. 168–9.
[59] Ceramics. Available from: http://www.ultramet.com/materials101.html.
[60] Liu L, Li HJ, Shi XH, Feng W, Wang YJ, Yao DJ. Effects of SiC addition on the ablation properties of C/C composites in different heat fluxes under oxyacetylene torch. Vacuum 2013;90:97–9.

[61] Liu L, Li HJ, Feng W, Shi XH, Wu H, Zhu JL. Effect of surface ablation products on the ablation resistance of C/C–SiC composites under oxyacetylene torch. Corros Sci 2013;67:60–6.
[62] Gallego NC, Edie DD. Structure–property relationships for high thermal conductivity carbon fibers. Compos Part A: Appl Sci 2001;32:1031–8.
[63] Fritze H, Jojic J, Witke T, Rüscher S, Weber S, Scheerer R, et al. Mullite based oxidation protection for SiC–C/C composites in air at temperatures up to 1900 K. J Eur Ceram Soc 1998;18:2351–64.
[64] Shi S, Liang J, Yi FJ, Fang GD. Modeling of one-dimensional thermal response of silica-phenolic composites with volume ablation. J Compos Mater 2013;47:2219–35.